

# SWIRLING FLOW IN CIRCULAR PIPES

by

MITSUKIYO MURAKAMI\* and OSAMI KITO\*\*

(Received May 28, 1976)

## Abstract

An analysis is given for swirl flows in straight pipes. The swirl and axial component of velocities can be expressed as functions of the swirl intensity, defined by the ratio of angular momentum flux to axial one. Experimental confirmation of the results is also given.

## 1. Introduction

Swirling flows resulting from pipe bends or fluid machines are found in many engineering practice and the flows received considerable attention from many researchers.

Seno<sup>(1)</sup> studied experimentally the effects of wall roughness on the decay of swirl flows in long circular pipes. Murakami<sup>(2)</sup> investigated experimentally the decay process of swirling flows in a straight pipe. Collatz<sup>(3)</sup> obtained analytical solutions for laminar pipe flows with weak swirling components. Lavan<sup>(4)</sup> also analyzed the same problem by using a perturbation method for small axial Reynolds numbers up to 20. Fully developed turbulent flows with weak swirl components were analyzed theoretically by Kreith.<sup>(5)</sup>

This paper gives results of an analytical investigation for turbulent swirl flows in circular pipes. The analysis was made on the assumptions that the space rate of change of velocity along the axial direction is negligible small as compared with that along the radial direction. The results obtained were confirmed by experiments.

## 2. Nomenclature

$p$  ; static pressure

---

\* Professor, Department of Mechanical Engineering, Nagoya University

\*\* Assistant, Department of Mechanical Engineering, Nagoya University

$Q$	; rate of discharge
$r$	; radial distance
$r_0$	; pipe radius
$Re$	; Reynolds number, $(=2r_0V_m/\nu)$
$V_m$	; mean axial velocity
$V_r$	; radial velocity
$V_z$	; axial velocity
$V_\theta$	; swirl velocity
$V_*$	; friction velocity
$y$	; distance from pipe wall
$z$	; axial distance
$\beta$	; decay exponent
$\epsilon_\tau$	; eddy viscosity
$\theta$	; flow angle in wall layer
$\lambda$	; friction factor
$\nu$	; kinematic viscosity
$\rho$	; density
$\tau_z$	; axial shear stress
$\tau_{zw}$	; value of $\tau_z$ on wall
$\tau_\theta$	; tangential shear stress
$\tau_{\theta w}$	; value of $\tau_\theta$ on wall
$\omega$	; angular velocity of vortex core
$\omega_z$	; vorticity component in $z$ direction
$\Omega$	; angular momentum flux or swirl intensity, Eq. (28)
$\Omega_0$	; value of $\Omega$ at pipe inlet

### 3. Equations of motion and solutions

The equations of motion and continuity under the conditions of incompressible fluid, and steady axi-symmetric flow are

$$V_r \frac{\partial V_r}{\partial r} + V_z \frac{\partial V_r}{\partial z} - \frac{V_\theta^2}{r} = -\frac{1}{\rho} \frac{\partial P}{\partial r} + \nu \left( r^2 V_r - \frac{V_r}{r^2} \right) \quad (1)$$

$$V_r \frac{\partial V_\theta}{\partial r} + V_z \frac{\partial V_\theta}{\partial z} + \frac{V_r V_\theta}{r} = \nu \left( r^2 V_\theta - \frac{V_\theta}{r^2} \right) \quad (2)$$

$$V_r \frac{\partial V_z}{\partial r} + V_z \frac{\partial V_z}{\partial z} = -\frac{1}{\rho} \frac{\partial P}{\partial z} + \nu (r^2 V_z) \quad (3)$$

$$\frac{1}{r} \frac{\partial}{\partial r} (r V_r) + \frac{\partial V_z}{\partial z} = 0 \quad (4)$$

For turbulent flows the equations of motion are obtained by adding eddy viscosity  $\epsilon_\tau$  to the kinematic viscosity in Eqs. (1), (2) and (3). From experimental results, it may be assumed that the space rate of change of velocity along the axial direction is sufficiently small as compared with the one along the radial direction and the pressure drop along the axial direction is nearly balanced by turbulent shear stress acting in that direction.<sup>(2)</sup> Under these assumptions Eqs. (2) and (3) can be simplified as follows,

$$V_r \frac{\partial V_\theta}{\partial r} + \frac{V_r V_\theta}{r} = (\nu + \varepsilon_{r\theta}) \left( \frac{\partial^2 V_\theta}{\partial r^2} + \frac{1}{r} \frac{\partial V_\theta}{\partial r} - \frac{V_\theta}{r^2} \right) \quad (2)'$$

$$0 = -\frac{1}{\rho} \frac{\partial P}{\partial z} + (\nu + \varepsilon_{rz}) \left( \frac{\partial^2 V_z}{\partial r^2} + \frac{1}{r} \frac{\partial V_z}{\partial r} \right) \quad (3)'$$

The general solutions of which can be written down as,<sup>(6)</sup>

$$V_\theta = \frac{c_1}{r} \int_0^r r \exp\left\{ \int_0^r \frac{V_r}{\nu + \varepsilon_{r\theta}} dr \right\} dr + \frac{c_2}{r} \quad (5)$$

$$V_z = \int_0^r \frac{1}{r} \int_0^r \frac{1}{(\nu + \varepsilon_{rz})} \cdot \frac{1}{\rho} \cdot \frac{\partial P}{\partial z} dr \cdot dr + c_3 + c_4 [l_n]_0^r \quad (6)$$

where  $c_1, c_2, c_3$  and  $c_4$  are integral constants.

### 3. 1. Swirl velocity distributions

With measured velocity distributions the velocity profiles within a pipe section can be divided into the three regions as

I ; the forced vortex region in the central zone of the section.

II ; the free vortex region in the annular zone of the section.

III; wall region near the pipe wall (in which wall shear stress dominates).

In the region I, the swirling velocity  $V_\theta$  tends to zero at the center and the integral constants in Eq. (5) becomes

$$c_1 \neq 0, \quad c_2 = 0$$

Velocity distributions near the wall do not follow the relation expressed by Eq. (5) but the wall law as given in Eq. (7), which was verified experimentally by

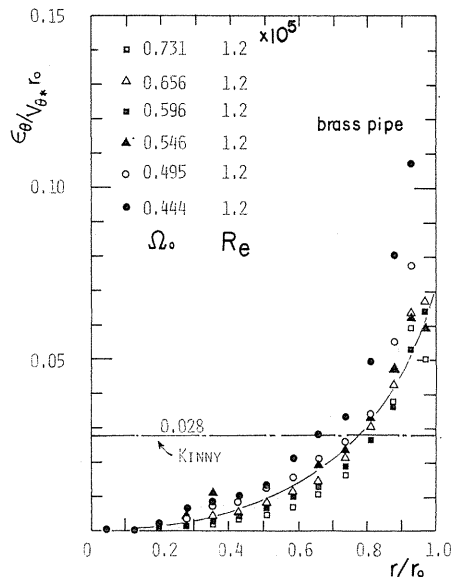


Fig. 1. Tangential component of eddy viscosity.

Backshall<sup>(10)</sup>. Consequently, in the region III, the velocity distribution can be expressed by

$$\frac{V_\theta}{V_*} = \frac{V \sin \theta}{V_*} = \left( A \log \frac{yV_*}{\nu} + B \right) \sin \theta \quad (7)$$

Equation (5) which is available for regions I and II contains a eddy viscosity  $\varepsilon_{\tau\theta}$ . The value of  $\varepsilon_{\tau\theta}$  is generally considered to depend on the flow velocities and its coordinates. Despite many investigations on the eddy viscosity  $\varepsilon_{\tau\theta}$ , any definite value of  $\varepsilon_{\tau\theta}$  has not been found. For simplicity's sake, many workers have been used the following simple expression for  $\varepsilon_{\tau\theta}$

$$\varepsilon_{\tau\theta}/r_0V_* = K \quad K = \text{const.} \quad (8)$$

Kinny<sup>(7)</sup> found the value of  $K$  to be 0.028 for a swirling flow between concentric cylinders, and Ragasdale<sup>(8)</sup> gave a value ranging from 0.038 to 0.08 for vortex type flow. The measured values of  $\varepsilon_{\tau\theta}$  in this investigation are plotted in Fig. 1. All the plots approximately fall on one curve irrespective of swirl intensity.

### 3. 1. 1. Weak swirl flow (in regions I and II)

When the swirl intensity is weak ( $\Omega < 0.2$ ), the swirl motion alters a little the profiles of axial velocity distributions and the rate of change of velocity profile along the pipe axis. In this case, the radial velocity calculated by the following relation

$$V_r = -\frac{1}{r} \int_0^r \frac{\partial(rV_z)}{\partial z} dr \quad (9)$$

is substantially zero. With this result, Eq. (5) can be integrated and gives

$$\text{for region I} \quad V_\theta = \frac{c_1}{2} r \quad (10)$$

$$\text{for region II} \quad V_\theta = \frac{c_1}{2} r + \frac{c_2}{r} \quad (11)$$

### 3. 1. 2. Strong swirl flow (in regions I and II)

When the swirl intensity is strong ( $\Omega > 0.2$ ), the axial velocity distribution has a concave profile at the center and this velocity profile decays in course of swirl decay. To check the order of the effect of  $Vr$  on the swirl velocity distribution, the maximum value of  $Vr$ , namely,  $\{Vr\}_{\text{max}}$  can be used. If a constant value of  $r_0\{Vr\}_{\text{max}}/\varepsilon_{\tau\theta} = k$  is assumed across the section, then Eq. (5) gives

$$V_\theta = \frac{c_1}{r} \cdot \frac{r_0^2}{k^2} \left\{ e^{\frac{k}{r_0} r} \left( k \frac{r}{r_0} - 1 \right) + 1 \right\} + \frac{c_2}{r} \quad (12)$$

The first term in the righthand side of this equation can be calculated numerically for several values of  $k$ , the results of which are shown in Fig. 2. As an example, a swirl flow of  $\Omega = 0.7$  is considered here. In this case, the following order estimation for  $Vr$  and  $\tau_{\theta w}$  can be made from the previous investigation<sup>(2)</sup>.

$$\frac{\{V_r\}_{\max}}{V_m} \sim \frac{1}{1000}, \quad \sqrt{\frac{\tau_{\theta w}}{\rho}} \sim \frac{V_m}{10}$$

If the value of  $K$  in Eq. (8) is assumed to be 0.03

$$k = \frac{r_0 \{V_r\}_{\max}}{k \cdot r_0 \cdot V_{\theta*}} = \frac{\{V_r\}_{\max}}{k \sqrt{\tau_{\theta w} / \rho}} \sim 0.3$$

With this result the graph of

$\frac{c_1}{r} \frac{r_0^2}{k^2} \left\{ e^{k \frac{r}{r_0}} \left( k \frac{r}{r_0} - 1 \right) + 1 \right\}$  plotted against radial distance give a forced vortex type distribution as shown in Fig. 2. Thus the relation of Eq. (12) can be taken to express the swirl velocity components in regions I and II in case of weak swirl intensity.

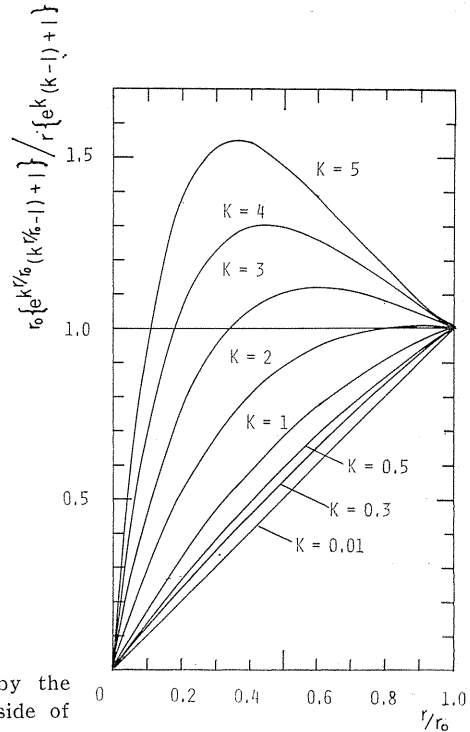


Fig. 2. Velocity profiles expressed by the first term of the righthand side of Eq. (12).

### 3. 1. 3. Swirl velocity distributions (in region III)

In the foregoing discussion it is assumed that the velocity distribution in region III can be expressed by Eq. (7). But the expression is only available in a fully turbulent region. Fully developed turbulent was attained for a flat plate at the distance from the wall  $y$  satisfying the relation  $\frac{yV_*}{\nu} \geq 70$ . Considering the effect of the centrifugal force in the swirl flow the condition of  $\frac{yV_*}{\nu} \geq 100$  is used here for fully turbulent and this condition gives  $y=2$  mm when  $Re=1.0 \times 10^5$  and  $\Omega=0.5$ . When pipe has a rough surface, the wall law becomes

$$\frac{V}{V_*} = A \log \frac{yV_*}{\nu} + B - \frac{\Delta V}{V_*} \quad (13)$$

where  $\Delta V/V_*$  depends on the size, shape and distribution of roughness elements. For fully rough surface  $\Delta V/V_*$  have the form

$$-\frac{\Delta V}{V_*} = 3.5 - 5.75 \log \frac{k_s V_*}{\nu} \quad (14)$$

where  $k_s$  is the size of roughness element.

If  $y^+$  denotes the distance from the wall surface at which fully turbulent is attained, the swirl velocity at this point is given by; for smooth pipe wall,

$$\frac{V \sin \theta}{V_*} = \left( 5.75 \log \frac{y^+ V_*}{\nu} + 5.5 \right) \sin \theta \quad (15)$$

$$\therefore V_{\theta}^+ = 17 V_* \sin \theta = 17 V_{\theta*} \sqrt{\sin \theta}$$

for rough pipe wall,

$$\begin{aligned} V_{\theta}^+ &= \left( 5.75 \log \frac{y^+ V_*}{\nu} + 5.5 - \frac{\Delta V}{V_*} \right) V_{\theta*} \sqrt{\sin \theta} \\ &= \left( 17 - \frac{\Delta V}{V_*} \right) V_{\theta*} \sqrt{\sin \theta} \end{aligned} \quad (16)$$

The following consideration will be available for  $y^+$  for rough surface. If the roughness Reynolds number  $\frac{k_s V_*}{\nu}$  is less than 100, the value of  $y^+$  may be determined from the relation,  $\frac{y^+ V_*}{\nu} = 100$ , and if the Reynolds number exceeds 100, it is reasonable to put  $y^+ = k_s$ , since the thickness of  $y^+$  determined from the equation  $\frac{y^+ V_*}{\nu} = 100$  will be merged in the roughness elements.

### 3.2. Axial velocity

The axial velocity distributions are given by Eq. (6), in which the constant  $c_4$  is taken to be zero, since the velocity at the pipe center should be finite. When the flow has no swirl component, static pressure is uniform across the section and pressure drop is given by

$$\frac{\partial P}{\partial z} = a_0 \quad (\text{const.}) \quad (17)$$

But when the flow has a swirl component the uniformity of the static pressure will be destroyed by the centrifugal force of the swirling motion and the pressure at any point in the section is given by

$$P = P_{\text{wall}} - \rho \int_r^{r_0} \frac{V_{\theta}^2}{r} dr \quad (18)$$

from which

$$\frac{\partial P}{\partial z} = \frac{\partial P_{\text{wall}}}{\partial z} - \rho \frac{\partial}{\partial z} \int_r^{r_0} \frac{V_{\theta}^2}{r} dr \quad (19)$$

To calculate the term  $\rho \frac{\partial}{\partial z} \int_r^{r_0} \frac{V_{\theta}^2}{r} dr$ , distribution of  $V_{\theta}$  and its decay along  $z$  direction must be known, but there is no theoretical provisions for it. For the sake of simplicity it is assumed that the value  $\partial p / \partial z$  changes linearly with  $r$  as

$$\frac{1}{\rho} \frac{\partial P}{\partial z} = a_0 + a_1 r \quad (20)$$

where  $a_0$  and  $a_1$  are constants.

Substituting the value of  $\partial p / \partial z$  in Eq. (20) into Eq. (6) and putting  $(\varepsilon_{rz} + \nu)$

to be a constant, Eq. (6) gives

$$V_z = \frac{1}{\epsilon_{\tau z+\gamma}} \left\{ \frac{a_0}{4} r^2 + \frac{a_1}{9} r^3 \right\} + c_0 \tag{21}$$

As the decay of swirl flow along the pipe is assumed to be small and variation of axial momentum flux is substantially negligible in the first approximation, the relation between pressure drop and wall shear stress can be written down as

$$2\pi \int_0^{r_0} \frac{\partial P}{\partial z} r dr = 2\pi r_0 \tau_{zw} \tag{22}$$

Equations (20) and (22) give the following relation,

$$\rho \left( \frac{a_0 r_0}{2} + \frac{a_1 r_0^2}{3} \right) = \tau_{zw} \tag{22}'$$

Now, rate of discharge is given as

$$Q = \pi r_0^2 V_m = 2\pi \int_0^{r_0} V_z r dr \tag{23}$$

from which

$$V_m = \frac{2}{\epsilon_{\tau z+\gamma}} \left\{ \frac{a_0}{16} r_0^2 + \frac{a_1}{45} r_0^3 \right\} + c_0 \tag{24}$$

Let  $V_z^+$  be the axial velocity  $V_z$  at  $y=y^+$ , then

$$V_z^+ = \frac{1}{\epsilon_{\tau z+\gamma}} \left\{ \frac{a_0}{4} r_0^2 + \frac{a_1}{9} r_0^3 \right\} + c_0 \tag{25}$$

where constants  $a_0$ ,  $a_1$ , and  $c_0$  in this expression can be determined if  $\tau_{zw}$ ,  $V_m$  and  $V_z^+$  are given.

Figure 3 indicates the results of authors experiment on  $\epsilon_{\tau z}$ . Plots of experimental points scatter rather widely, but in the past any authorized values of  $\epsilon_{\tau z}$  have not been published.

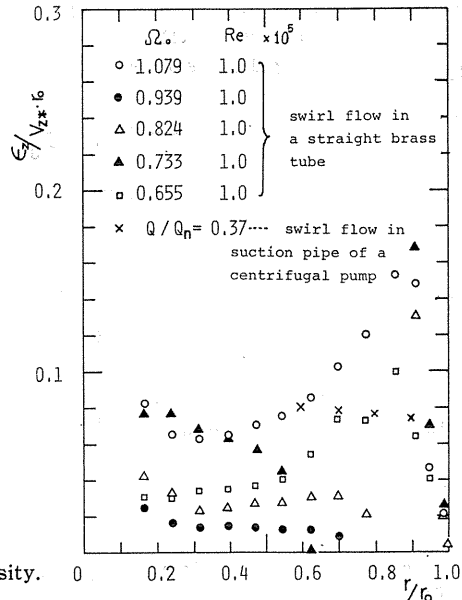


Fig. 3. Axial component of eddy viscosity.

### 3. 3. Flow angle near wall

Flow angles in the wall layer are defined by the following equation

$$\tan \theta = \frac{(V_\theta)_0}{(V_z)_0} \quad (26)$$

where  $(V_\theta)_0$  and  $(V_z)_0$  are the swirl and axial components of flow in the wall layer. This flow angle  $\theta$  changes with the swirl intensity  $\Omega$ . If it is assumed that the axial velocity component  $(V_z)_0$  is independent of the swirl one, the functional relation between  $\theta$  and  $\Omega$  can be given as follows

(i) for forced vortex distributions

$$\begin{aligned} \frac{V_\theta}{V_m} &= \omega \left( \frac{r}{r_0} \right) \\ \therefore \tan \theta &= \omega / \left\{ \frac{(V_z)_0}{V_m} \right\} = \omega \quad (\because V_z = V_m) \end{aligned} \quad (27)$$

In this case dimensionless expression of angular momentum flux becomes

$$\begin{aligned} \Omega &= 2\pi\rho \int_0^{r_0} V_z V_\theta r^2 dr / \rho\pi r_0^3 V_m^2 \\ &= 2 \int_0^1 \omega \left( \frac{r}{r_0} \right)^2 d \left( \frac{r}{r_0} \right) = \frac{\omega}{2} \end{aligned} \quad (28)$$

$$\therefore \tan \theta = 2\Omega \quad (29)$$

(ii) for forced-free vortex distributions

$$\begin{aligned} \frac{V_\theta}{V_m} &= \omega \left( \frac{r}{r_0} \right) + c \left( \frac{r_0}{r} \right) \\ \therefore \tan \theta &= \omega + c \end{aligned}$$

and hence angular momentum flux is given by

$$\Omega = 2 \int_0^1 \left( \omega \left( \frac{r}{r_0} \right)^3 + c \left( \frac{r}{r_0} \right) \right) d \left( \frac{r}{r_0} \right) = \frac{\omega}{2} + c$$

From above results, the following relation can be obtained

$$\tan \theta = \Omega + \frac{\omega}{2} \quad (30)$$

This relationship between  $\tan \theta$  and  $\Omega$  may be confirmed by experiments as shown in Fig. 4. But the numerical factors in Eqs. (29) and (30) differ slightly from those assumed by experimental results, which will probably due to the rough assumption on the axial velocity  $(V_z)_0$ ,  $((V_z)_0 = V_m)$ .

To meet with experimental results, Eqs. (29) and (30) are rewritten with altered numerical factors as



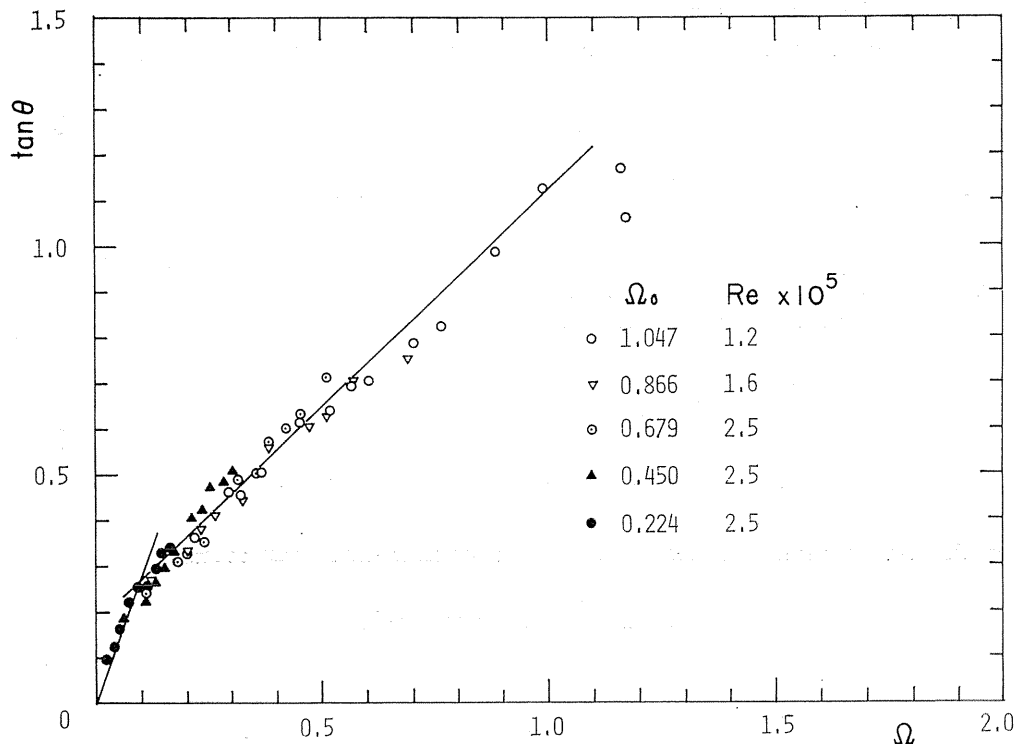


Fig. 4. Relation between  $\tan \theta$  and  $\Omega$  (brass pipe).

$$(i) \quad \tan \theta = 2.7\Omega \quad (29)'$$

$$(ii) \quad \tan \theta = 0.95\Omega + 0.17 \quad (30)'$$

#### 4. Experimental results

##### 4. 1. Vorticity distributions

Distributions of vorticity component  $\omega_z$  in  $z$  direction across several sections are shown in Fig. 5, where  $\omega_z$  is defined by

$$\omega_z = \frac{1}{r} \frac{\partial}{\partial r} (rV_\theta) \quad (31)$$

Except the inlet region ( $s_1 \sim s_5$ ) and the sections with weak swirl ( $\Omega < 0.1$ ),  $\omega_z$  has approximately a constant value within the region  $0.6 < r/r_0$ . The constant value is 0.4 for brass pipes and 0.3 for steel pipes. Within the core region  $0 < r/r_0 < 0.6$ , the values of  $\omega_z$  change with radial distance ( $r/r_0$ ) and swirl intensity  $\Omega$ . When  $\Omega < 0.1$ ,  $\omega_z$  remains nearly constant over the cross section. When the swirl intensity  $\Omega$  is greater than 0.1, the swirl velocity distributions within the range  $0.6 < r/r_0$  can be expressed as

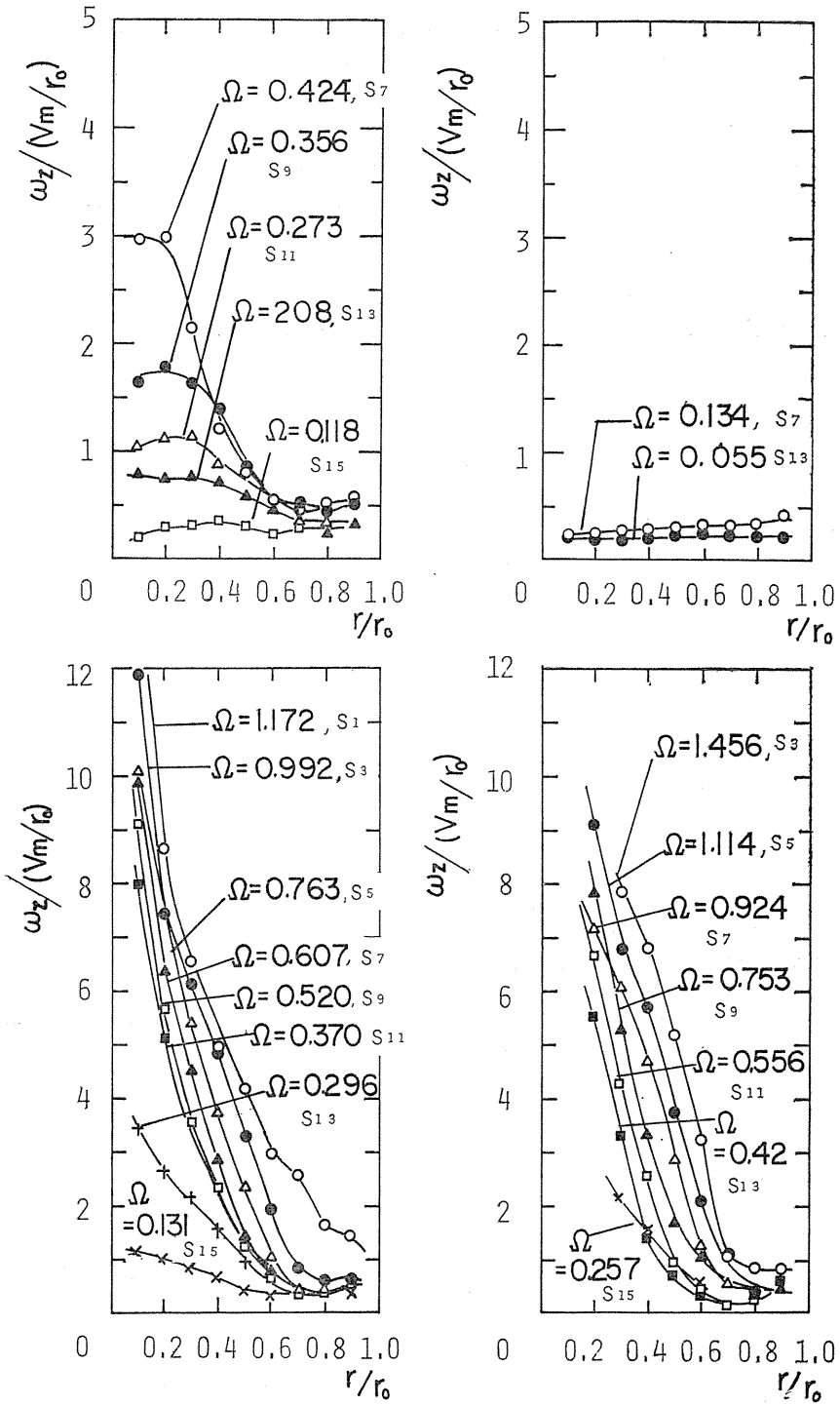


Fig. 5. Distributions of vorticities.

$$V_\theta = \frac{1}{2}\omega_z r + \frac{c}{r} \tag{32}$$

where  $\omega_z$  is independent on swirl intensity.

This equation shows that the swirl velocity can be expressed as the sum of velocities due to a forced vortex motion of strength  $\frac{1}{2}\omega_z$  and a free vortex motion of arbitrary intensity. This result agrees with the analytical results for region II described in section (2.1). It should be noted that when  $\Omega > 0.1$ , the value of  $\omega_z$  is a universal constant. Consequently, the decay phenomenon of swirling flow appears only in the component of the free vortex motion.

If the swirl intensity is weak and  $\Omega < 0.1$ ,  $V_\theta$  can be given as

$$V_\theta = \frac{1}{2}\omega_z r \tag{33}$$

since  $\omega_z$  is substantially constant over the section, and  $(V_\theta)_{r=0} = 0$ .

#### 4. 2. Swirl velocity

The following model for the swirl velocity can be given, from the above considerations

$$\frac{V_\theta}{V_m} = a\left(\frac{r}{r_0}\right) + bf\left(\frac{r}{r_0}\right) \tag{34}$$

The first term of the righthand side of Eq. (34) expresses a forced vortex motion and the second term a free vortex one. The value of  $f\left(\frac{r}{r_0}\right)$  in Eq. (34) can be calculated from measured velocities as is shown in Fig. 6. The experimental results can be shown by one curve irrespective of different swirl intensities. Numerical factors  $a$  and  $b$  in Eq. (34) depend on swirl intensity  $\Omega$ , and their relationships are shown in Figs. 7 and 8. The results within the inlet region are excluded in these figures. When  $0.1 < \Omega$ ,  $a$  is nearly constant, the value of which is 0.18 for brass pipe and 0.12 for steel pipe. When  $\Omega < 0.1$ ,  $a$  decreases as  $\Omega$  reduces, and becomes zero at  $\Omega = 0.1$ . From the above considerations, it may be concluded that the swirl velocity can be expressed as the sum of a forced vortex motion and a free vortex one if  $\Omega$  exceeds 0.1, and as a

$\Omega_0$	Re $\times 10^5$
○ 0.721	1.2
● 0.505	1.2
△ 0.470	1.2
▲ 0.357	1.2
○ 0.208	2.5
□ 0.241	2.5
■ 0.356	2.5
× 0.396	2.5
+ 0.485	2.5

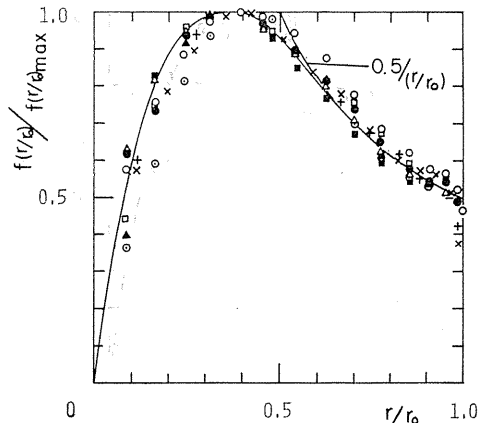


Fig. 6. Curve of  $f(r/r_0)$  in free vortex range.

forced vortex if the value of  $\Omega$  is less than 0.1.

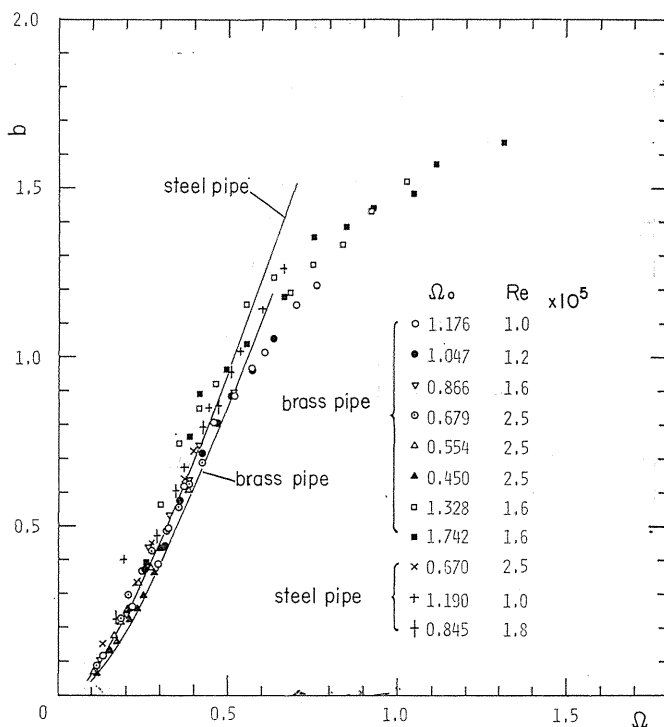


Fig. 7. Relation between  $b$  and  $\Omega$ .

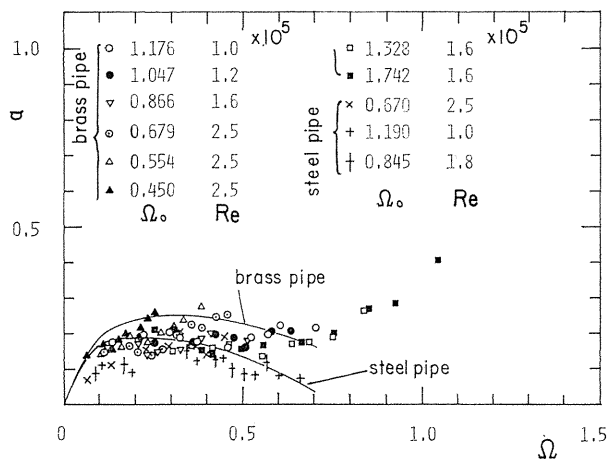


Fig. 8. Relation between  $a$  and  $\Omega$ .

### 5. Experimental verification of calculated results

As the first step, the flow next to the wall or in region III is considered. The distance from the wall at which the fully turbulent is attained is so small that, the

concept of wall slip may be introduced. The wall slip condition is given by

$$\frac{V_{\theta}^+}{V_m} = a \left( \frac{r_0}{r_0} \right) + bf \left( \frac{r_0}{r_0} \right) = a + bf(1) \quad (35)$$

In this case the angular momentum flux becomes

$$\Omega = 2 \int_0^1 \left\{ a \left( \frac{r}{r_0} \right) + bf \left( \frac{r}{r_0} \right) \right\} \frac{V_z}{V_m} \cdot \frac{r^2 dr}{r_0^3} \quad (36)$$

From Eqs. (35) and (36), the values of  $a$  and  $b$  can be determined as functions of  $\Omega$  if  $V_{\theta}^+$  is given. With the condition  $\frac{y^+ V_*}{\nu} = 100$  Eq. (7) gives

$$V_{\theta}^+ = 17V_* \sin \theta = 17V_{\theta*} \sqrt{\sin \theta} \quad (37)$$

where

$$V_{\theta*} = \sqrt{\frac{\tau_{\theta w}}{\rho}}$$

It is known that  $\Omega$  decays exponentially downstream<sup>(2)</sup>, and hence the shear stress  $\tau_{\theta w}$  may be expressed as

$$\frac{\tau_{\theta w}}{(\rho V_m^2/2)} = -\beta \Omega \quad (38)$$

where  $\beta$  is a decay exponent.

For brass pipe, by taking the value  $\beta$  to be 0.011,  $V_{\theta}^+$  can be determined by use of Eqs. (29)' and (30)'. To estimate the value of  $V_{\theta}^+$  for steel pipe having a rough surface, Eq. (13) should be used instead of Eq. (7), in which it is assumed that  $\Delta V/V_* = 7$ , because  $\frac{k_s V_*}{\nu}$  is nearly equal to 65 for steel pipe.<sup>(9)</sup>

The tangential stress of steel pipe can be calculated with the use of a friction factor  $\lambda$  by

$$(\tau_{\theta w})_{\text{steel}} = \frac{\lambda_{\text{steel}}}{\lambda_{\text{brass}}} (\tau_{\theta w})_{\text{brass}}$$

The calculated values of  $V_{\theta}^+$  are indicated by solid lines in Fig. 9. If these values are used in Eqs. (35) and (36) the constants  $a$  and  $b$  can be determined as shown by solid lines in Figs. 7 and 8, in which it is assumed that  $V_z/V_m = 1.0$  for simplicity's sake. An experimental agreement is confirmed within the region  $0 < \Omega < 0.6$ . When  $\Omega$  increases beyond 0.7, the discrepancy increases, which will be due to the defect of the assumption of  $V_z$ . Namely, the assumption that  $V_z/V_m = 1.0$  will lose its validity.

To find the axial velocity distribution, Eqs. (23), (24), (25) and (26), as well as Eq. (39) can be used.

$$\left. \begin{aligned} V_z^+ &= V_{\theta}^+ / \tan \theta \\ \tau_{zw} &= \tau_{\theta w} / \tan \theta \end{aligned} \right\} \quad (39)$$

As an example, calculated results for a smooth pipe is shown in Fig. 10, in which the measured values are also plotted. Agreement is satisfactory except the wall region.

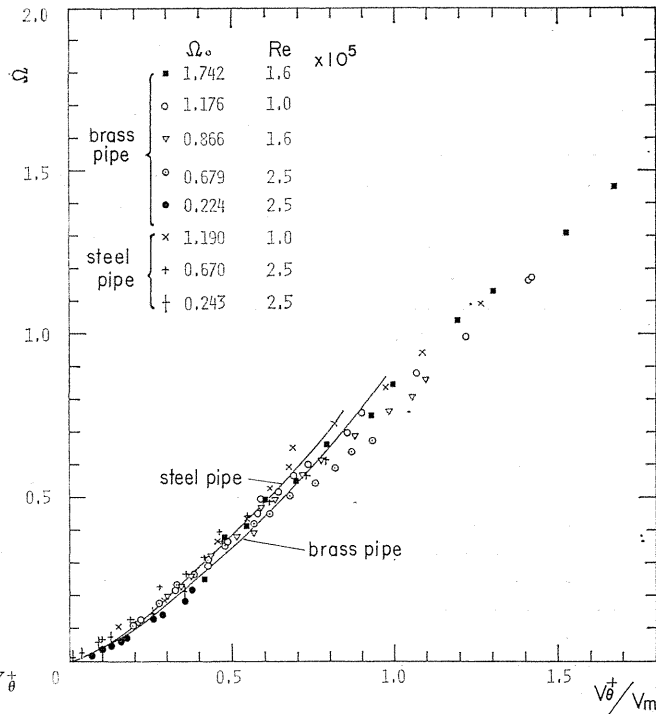


Fig. 9. Relation between  $V_{\theta}^+$  and  $\Omega$ .

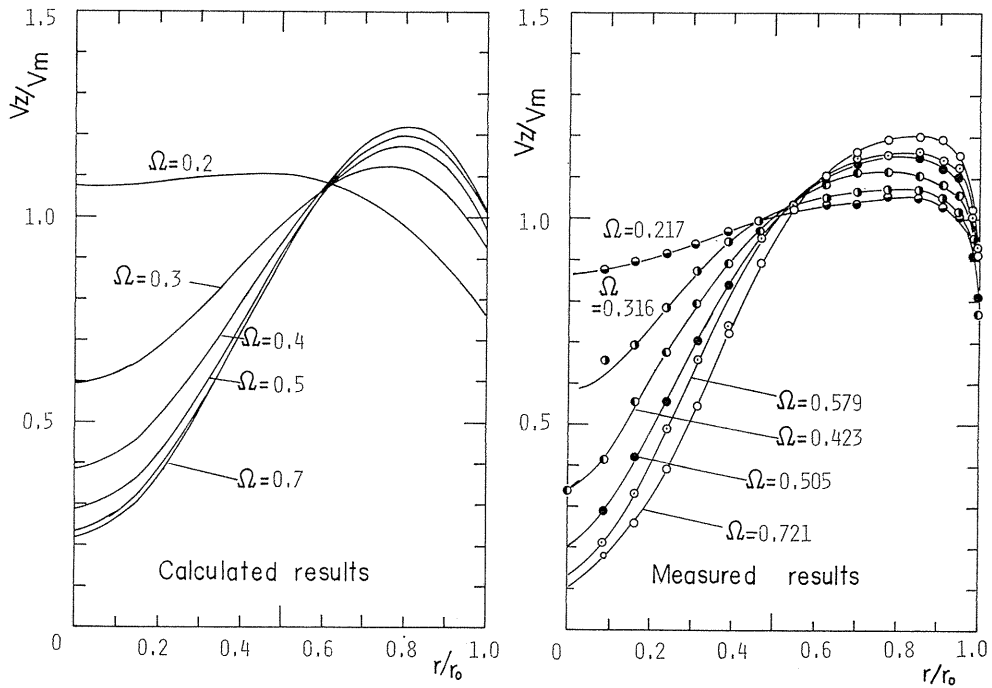


Fig. 10. Distributions of axial velocities.

### 5. Conclusions

1. The swirl velocity is generally expressed as the sum of velocities due to a forced vortex motion and a free vortex one.
2. When  $\Omega$  exceeds 0.1, the decay of the swirl velocity follows the same process as the free vortex motion and the forced vortex component remains unaltered. When  $\Omega$  is less than 0.1, the decay of the swirl velocity follows the same process as the decay of the forced vortex motion.
3. Axial velocities can be calculated by equating the pressure drop along pipe axis to the turbulent axial stress.

### References

- (1) Seno, Y. and Nagata, T., Bull. JSME., Vol. 15, No. 90, (1972), P. 1514.
- (2) Murakami, M., et al., Bull. JSME., Vol. 19, No. 128, (1976), P. 118.
- (3) Collatz, L., and Görtler, H., Z. Angew. Math. u. Phys., Vol. 5, (1954), P. 95.
- (4) Rochino, A. P. and Lavan, Z., Trans. ASME., Ser. E, Vol. 36-2 (1969-6), P. 151.
- (5) Kreith, F. and Sonju, O. K., J. Fluid Mech., Vol. 22, part 2, (1965), P. 257.
- (6) Einstein, H. A. and Li, H., Steady Vortex Flow in a Real Fluid. Heat Transfer and Fluid Mechanics Institute, Stanford Univ. Press, (1951).
- (7) Kinny, R. B., Trans. ASME., Vol. 89, Ser. E, June 1967, P. 437.
- (8) Ragasdale, R. G., NASA TND-1051, 1961.
- (9) Clauser, F. H., Advances in Applied Mech. Vol. 4(1956), Academic Press.
- (10) Backshall, R. G. and Landis, F., Trans. ASME., Ser. D, Vol. 91 (1969-12), P. 728.